Proc. of SPIE Vol. 3130, Lens Design, Illumination, and Optmechanical Modeling, ed. R E Fischer, R Johnson, R C Juergens, W J Smith, P (Sep 1997)

Unified thermal/elastic optical analysis of a lithographic lens

Alson E. Hatheway

Alson E. Hatheway Inc.
Suite 400
595 East Colorado Boulevard
Pasadena, California 91101
(626) 795-0514

ABSTRACT

Lithographic lenses often exhibit shifts in focal position and magnification due to the influence of the heating transient initiated when the illuminator is turned on. Evaluation of these effects requires simultaneous solution of the equations of heat transfer, elasticity and optical images. "Unified" analysis techniques were used, including the Optical Analog™, which provide accurate analysis of the influence of all the design variables on the optical image. This paper describes the modeling process in detail as well as the checkout techniques used to assure that the physics of the problem had been adequately captured in the model. The paper closes with a discussion of some of the valuable insights that were gained during the analysis.

Key Words: integrated analysis, unified analysis, thermal/elastic, optomechanics

1.0 INTRODUCTION

Recent years have witnessed a dramatic increase in the interest in multidisciplinary analysis. The optical industry has been particularly active in developing techniques to understand and predict the temporal and thermal behavior of systems ranging from astronomic telescopes to laser cavities and even to optical fiber couplers. The analyses often include optical physics, structures to support them (elasticity), the steady-state and transient heating, aerodynamic buffeting and many other fields or disciplines. One vehicle often used for these analyses is called "Integrated" analysis and it allows each field or discipline to work in its own software while the Integrated Analysis data base manager moves the data around from code to code while reformatting output of one code to be input to another code and interpolating (or extrapolating) data values to fit the geometric requirements at the software interfaces.

Each of the codes is run sequentially and the timing, formatting and interpolation are performed by the data base manager. The handicaps of this analysis approach have been discussed elsewhere[5].

"Unified" analysis techniques were used in the analyses described here. These analyses incorporate all the disciplines into one data base and the analyses are run in one analysis code. The equations of the disciplines are then incorporated into one matrix array for simultaneous solution. Figure 1 shows the organization of the model building activity and Figure 2 shows the

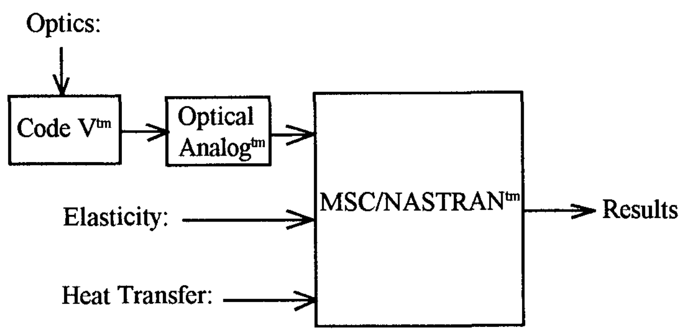

Figure 1. Unified analysis process

distribution of disciplines in such a Unified analysis matrix.

The advantages of Unified analysis are speed, economy and accuracy. By having all the data in a single model's data base it is possible to make revisions quickly and turn the analysis around economically. Additionally, since all the data is in a shared data base it must all share the same geometry, thereby eliminating interpolation and extrapolation errors. The resulting analyses are all performed in a single pass through the computer and the results are quickly available.

MSC/NASTRAN™ was selected as the analysis code for the Unified model. It explicitly supports a number of analogies to elasticity (thermal conduction, radiation and servo-control systems) and through its open architecture and constraint equations is adaptable to implicit analogies such as optical rays, acoustics, and magnetic fields.

The lithographic lens that was the subject of this analysis is shown in Figure 3. It had seventeen

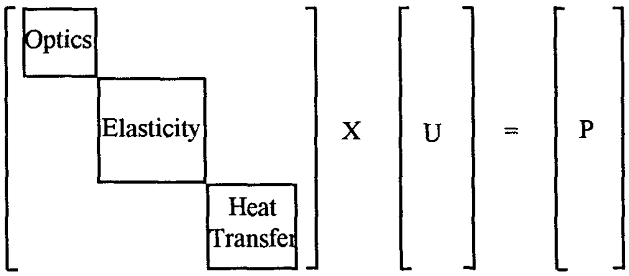

or:

[Influence Coefficients] X [Response] = [Loading]

Figure 2. Unified analysis formulaltion.

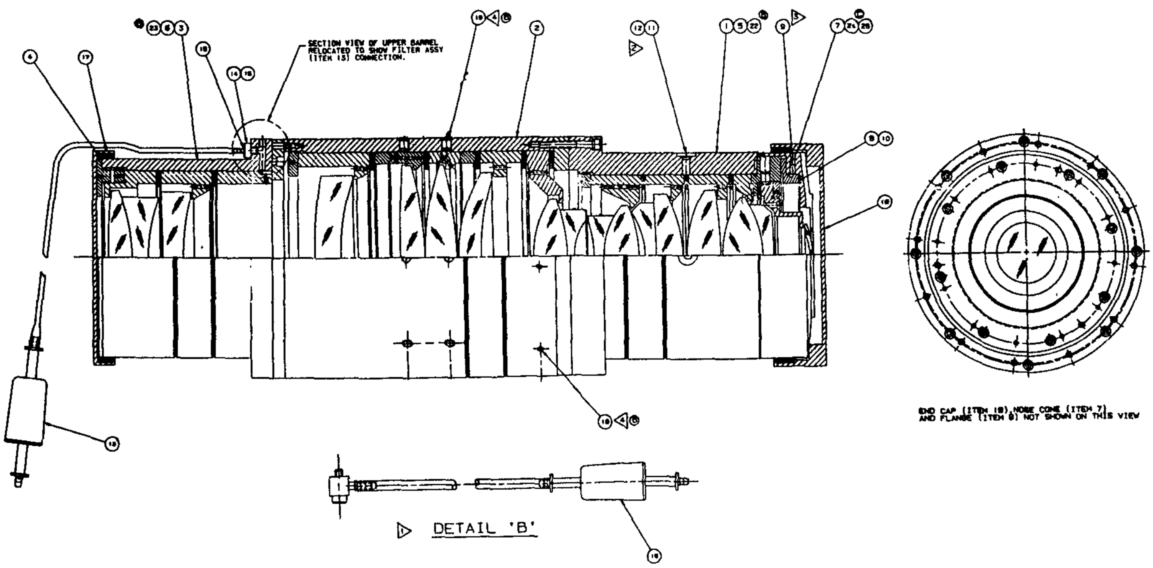

Figure 3. The lithographic lens assembly.

glass lenses including five cemented doublets.

2.0 MODEL DEVELOPMENT

A Unified model may include as many disciplines as necessary to capture the physics of the problem to be solved. In this case the disciplines are heat transfer, elasticity and optical imaging and the modeling activity must plan to accommodate the needs of each of these:

Heat transfer-
The lens assembly is heated by the conversion of radiant illumination (ultraviolet light) into heat by the process of absorption. The absorption occurs as a volumetric phenomenon (lenses absorb power as the light transits them). Furthermore, the lens is cooled by natural convection to ambient air on its outside perimeter surfaces. The heat must be conducted and convected (the lens' air spaces are filled with nitrogen) from the location at which the heat is absorbed to the outside surfaces at which the natural convection cooling is occurring.

Elasticity-
The lenses are bonded into stainless steel cells with an elastomeric polymer and the cells are then clamped into the tubular housing with threaded retaining rings. The lens assembly is mounted vertically on a circumferential ring which positions it with respect to the image plane (wafer) and the object plane (mask). The elastic model must not only capture the elastic behavior of each component (lens, cell, etc.) but also capture the interaction between them as they change shape and size under the influence of temperature changes.

Optical Image Formation-
Both changes in temperature and changes in geometry of the lenses will influence the position, size and quality of the optical image. In predicting these changes using ray tracing techniques it is the local properties (temperature, translation, rotation, strain) at each of the ray intercept points that determines the refractive behavior of the ray at that point. It is therefore important that the model incorporate the surface properties at each of the ray intercept points and that the analysis calculate the changes in these properties at these points.

The lens assembly was designed with rotational symmetry in both the optical and mechanical aspects and since the lens is used with its optical axis oriented vertically it was only necessary to model a 90° sector of the lens and apply symmetrical constraints at the free edges.

The modeling effort began with a definition of the optical features (rays and ray intercept points) that would be used to evaluate the changes in the optical image. Seven rays were selected representing seven equal zones at the aperture stop. Each ray therefor represented equal illumination power at the image and each would contribute equally to the changes in focal point and image size. The seven rays were analyzed by Code V^{tm} to determine their surface-by-surface data (angles of incidence, intercept heights, etc.). The Code V plot of these rays is shown in Figure 4.

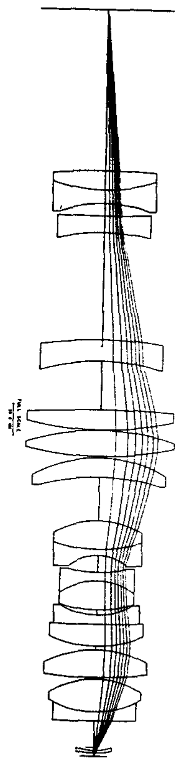

Figure 4. A Code V ray trace of the lithographic Lens, in the operating position.

Code V's tabular output data was then run through a computer program that converted its surface-by-surface data into finite element form (XYZ locations for GRID points at the ray intercept points and PLOTEL elements to connect the ray intercept points and trace the rays in MSC/NASTRAN). The same computer program was used to define the elastic solid elements for each of the lens elements. This procedure assured that the ray intercept points were congruent with the GRID points that defined the nodes of the solid elements and define the thermal/elastic behavior of the glasses. This congruence provides the highest accuracy in calculating the interaction between the thermal/structural model and the optical rays.

The computer program also wrote constraint equations into MSC/NASTRAN format that made the rays' positions and orientations dependent upon the translations, rotations and temperature at each of the ray intercept points. These equations were derived from the Code V optical prescription data at the same time as the optical rays and optical elements were generated from the surface-by-surface data. The computer program generates these equations through analogies between the optical behavior being modeled and the analysis discipline (elasticity) in the code being used. The program is called the Optical Analog^{tm} Program. The program incorporates additional elements to simulate the sensitivity of the index of refraction to temperature, dn/dT. This Optical Analog model is shown in Figure 5.

The constraint equations were also used to calculate (in MSC/NASTRAN) the change in the position of best focus and the change in magnification of the lens.

The thermal/elastic model of the optical elements was further influenced by the need to accurately simulate the distribution of the absorbed heat in each of the lenses.

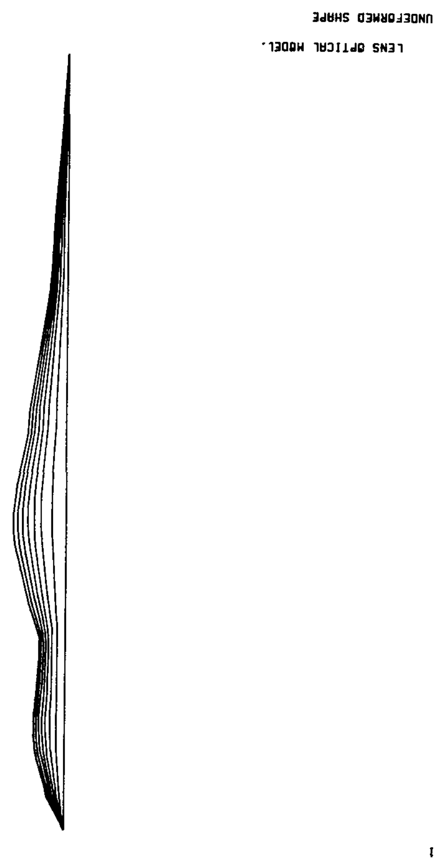

Figure 5. The Optical Analog^{tm} model of the optical rays in MSC/NASTRAN, in the operating position.

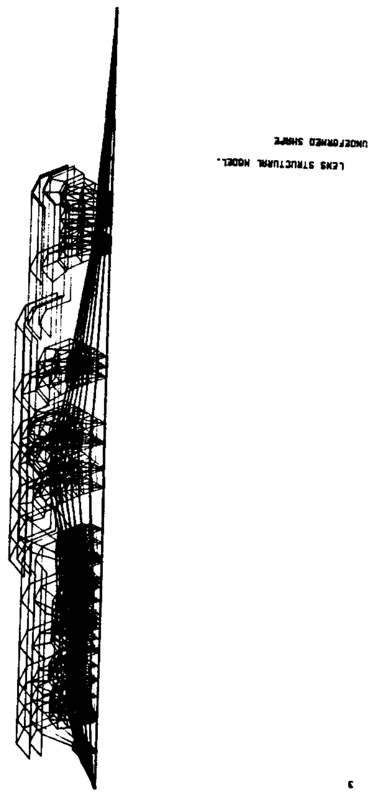

Figure 6. The Unified thermal/elastic optical model in the lens's operating position.

The image and object points being analyzed were on the optical axis and therefore the ray intercept points for may of the lenses were also near the axis. However, the real object (mask) is extended so that heating is widely distributed in most of the lenses and this required additional structural detail in most of the lenses that was outside the zones of the axial ray bundle. This additional detail allowed the "tailoring" of the ultraviolet flux intensity at each of the lenses to more nearly simulate the actual distribution of the heat power dissipation in the lenses.

The stainless steel cells and lens assembly structure were then modeled to support the lens elements and the optical rays in the appropriate position. The cells and lens structure were modeled as shell elements. In order to achieve displacement errors of about three percent the cells and tubular structure were modeled with three elements spanning the 90° (symmetrical) sector and fourteen elements spanning the length of the tube. The three percent error in the model was estimated from similarity to the Scordelis-Lo roof problem[3]. The Unified thermal/elastic optical model is shown in Figure 6.

3.0 MODEL VALIDATION

The resulting thermal/elastic optical model was validated in two ways. First it was compared to Code V results for simple cases which they could both analyze; lateral magnification and thermal soak of the glass elements (only).

The lateral magnification check was first performed by translating the object point in the lateral directions and observing the resulting translations of the image point as calculated by the Optical Analog model. The results were compared to the known magnification of the lens assembly, 1/5, and are shown below:

Axis:	Magnification:	
	Optical Analog:	Code V:
X	.19955	0.200
Y	.19966	0.200

The coefficients used in the constraint equations by the Optical Analog were limited to three significant figures, consistent with the observed accuracy of the calculations. Greater precision may be achieved if double-field card images are used in the finite element code.

The thermal soak response validation submitted both the Code V model and the Optical Analog model to a 1.0 C degree increase in temperature. The coefficients for thermal expansion of both the cement and the stainless steel were set to zero in the Optical Analog model in order to test only the refractive behavior of the glass elements. The results were compared:

Method:	Change in Position of Best Focus:
Code V	0.77×10^{-6} meters
Optical Analog	0.7684×10^{-6} meters

The validation exercise indicated that the Optical Analog model appropriately modeled both the refractive properties of the glasses and their sensitivity to changes in temperature, dn/dT.

As a second validation exercise on the Unified optomechanical model it was subjected to a uniform 1.0 degree C temperature increase. This exercise included the thermal expansion effects of the cement and stainless steel and the elastic interactions among all portions of the lens assembly model. In this validation exercise we discovered that the structures that support the object (the mask) and the desired image plane (the wafer) participate in the change of focus and magnification; that is, the mask, which is the primary heat-block in front of the lens, absorbs some heat and its support structure expands accordingly, changing the mask's position. Likewise, the focus shift was measured from the wafer surface whose supporting structure responds to the scattered and absorbed heat from the focal plane. Detail modeling of these structures were deemed to be beyond the scope of the current task. Simple bar elements were incorporated to simulate these structures and the agreement was improved. The adequacy of this simulation was not separately validated.

Although Code V was not able to provide solutions on this problem, it was possible to test an actual lens assembly and compare the unified model results against the actual test data:

Thermal Soak Method:	Focus Shift: (microns)
Test	0.5
Unified Analysis	0.87

This discrepancy (0.87 from the analysis versus 0.5 from test) appears to be an artifact of the uniform ΔT thermal load and the decision that a 3% residual error in the elastic model was acceptable. This effect is discussed further in the conclusions.

4.0 TRANSIENT PERFORMANCE ANALYSIS

The first step was to develop the heat loads in the lens assembly. It was assumed that a total continuous beam power of 1.0 watt was incident at the first surface of the first lens. The heat absorbed from the beam by each lens was calculated based upon the absorption coefficient for each lens's material, the beam's intensity at the lens and the lens' thickness. About seventy percent of the beam's power was delivered to the object plane, the wafer. At the wafer it was assumed that forty percent of the incident power was reflected specularly and returned to the optical system, transiting in the opposite direction. In all, about thirty-eight percent of the 1.0 watt initial beam power was absorbed by the glasses in the lenses. This included a small amount absorbed by the adhesives in the cemented doublets. This was the only source of heating considered in the analysis.

Initially, this power dissipation was distributed uniformly in the central area of each lens, an area representing about fifty percent of the surface area of the subject lens.
The amplitude of the resulting focus shift after sixty minutes of exposure was very small, about -300. nanometers compared to the anticipated -5.5 microns.

Heat Distributed Uniformly Over Central Area	Focus Shift (microns)
Test	5.5
Unified Analysis	-0.300

Subsequently, a detailed analysis of the radiant intensity at each lens surface disclosed power distributions (radially) that were considered to be more representative of the actual conditions in a lens during service than the initial assumption, above. The heat loading in the Unified analysis model was revised to represent more nearly the "bell-shaped" distributions that this analysis disclosed. This involved, in most cases, moving more heat out (radially) toward the margins of the lenses. The peak power on-axis was increased in some cases and reduced in others. The total heating (absorbed power) was unchanged.

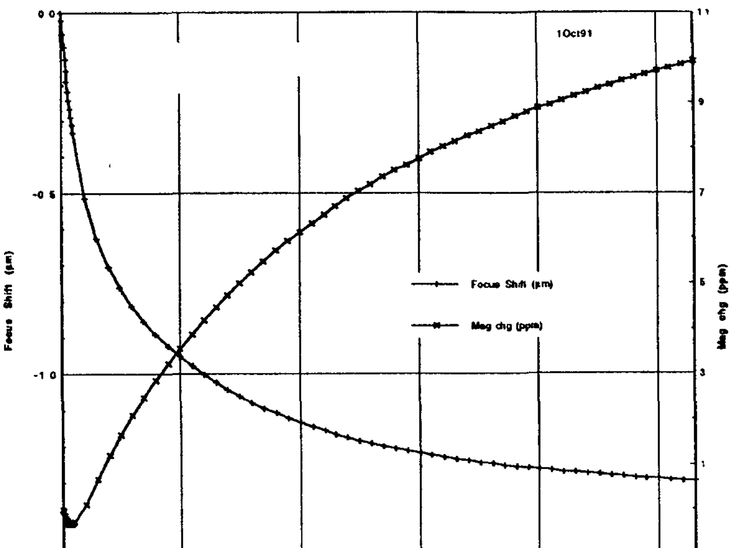

Figure 7. The transient changes in focus position and magnification as calculated by the Unified model.

A rerun of the transient analysis showed a pronounced increase in the magnitude of the focus change; -1.23 microns after

60 minutes of exposure. Figure 7 shows the calculated history of the focus shift and the concurrent magnification change resulting from the redistributed radiant flux in the optical beam in the lens.

"Bell-Shaped" Heat Distribution

	Focus Shift (microns)
Test	-5.5
Unified Analysis	-1.23

The fourfold increase in the focus shift effect was due entirely to a change in the assumed distribution of the optical radiation in the lens assembly. The net heating power and all the other modeling parameters were unchanged.

It is not clear that this heat distribution was the appropriate one for the conditions being simulated; it appears to have been based upon a 104 mm. square mask (object) whereas the tests were performed with a 15 mm. square mask. Considering the sensitivity of the response to the heat distribution this could account for the factor of about four between the analysis data and the test data.

5.0 DISCUSSION

The data presented above permit us to make some observations about the ease of making accurate models of the various phenomena involved in the unified analysis.

5.1 Optical Analog model accuracy

The first set of data involved the incorporation of the optical rays and the laws of refraction, including thermal sensitivities, into the finite element code (the Optical Analog model). In both rigid-body motions and uniform temperature excursions the Optical Analog model agreed very well with the expectations of optical physics as embodied in the lens design code, Code V. Dividing the Optical Analog response by the Code V response we may determine a figure of accuracy, FA for the Optical Analog calculation:

$$FA_{OA/CV}=\text{Optical Analog/Code V}=.19955/.200=.9977\ .$$

This figure of accuracy says that the Optical Analog model captured 99.77% of the expected physical effect. As discussed above this is consistent with the three significant figure format of the coefficients used in the calculation.

The Optical Analog's response to a uniform temperature rise tests the implementation of the thermal expansion and dn/dT behavior of the lenses. The calculation of a figure of accuracy for this case yields,

$$FA_{OA/CV}=\text{Optical Analog/Code V}=.7684/.77=.9979$$

which is virtually the same as for the magnification test.

These results show that it is practical and effective to incorporate the optical laws into a finite element model. Over the range of displacements usually encountered in mechanical work the optical laws are well represented by linear approximations suitable for inclusion in finite element models; in the present case, the linear finite element representation of the focus and magnification changes was accurate to within one-quarter of one percent or better. This accuracy is typical of Optical Analog models.

5.2 Unified elastic optical model accuracy

Calculating a similar figure of accuracy for the 1 0 degree C uniform temperature rise for the full Unified model,

$$FA_{OM/TD}\text{=Optomechanical Model/Test Data=.87/.50=1.74 .}$$

The full optomechanical model appears to capture 174% of the expected optical behavior, that is the optical response is 74% too large, compared to the test data. To understand how our elastic model influences the formation of an image we must consider that the effect at the image is the sum of each of the effects at each surface. Since the lens assembly has 29 free surfaces (17 glass elements including five cemented doublets) to influence the image and we estimated that each of these surfaces was determined to about three percent residual error, the net error at the image could be as large as

$$\text{net error} = 29 \times .03 = .87,$$

in which case

$$FA_{OM/TD}=1.87,$$

if the errors act systematically in the same direction. This provides an estimate of the upper bound of the accuracy of the model's image properties. Our observed error of 74% is within the upper bound and suggests that the model's geometry and the uniform temperature loading tend to make the errors sum systematically rather than randomly.

These data show that accuracy planned into the elastic model does not transfer directly to an optical response modeled by the Optical Analog. The analyst needs to divide the allowable error in the image characteristics by the number of surfaces that the rays transit and this smaller allowable error becomes the requirement on the elastic model. Typically, the analyst controls the accuracy of his model by increasing or decreasing the mesh size used to define the elements. More elements (smaller mesh size) improves the accuracy quite quickly; halving the mesh dimension reduces the errors by a factor between six and seven.

5.3 Unified thermal/elastic optical model accuracy

Figures of accuracy may also be calculated for each of the transient heating conditions. For the first analysis using a simplified heat distribution the focus shift was calculated to be -300 nm. so that

$$FA_{(ThE/TD)1}=-.300/-5.5=.055 .$$

The second analysis with a bell-shaped distribution resulted in a focus shift of -1.23 microns and

$$FA_{(ThE/TD)2}=-1.23/-5.5=.22$$

for a fourfold increase in the influence of the heating on the position of the image.

It is an axiom in heat transfer analysis that the greatest uncertainty is the heat load. In thermal/elastic analysis the axiom may be restated, "the greatest uncertainty is the heat load distribution." The uncertainty in the magnitude of the thermal load is compounded by an uncertainty in the location of the load and accurate knowledge of both is necessary in order to calculate the strain gradients that cause the deflections.

5.4 Advice to the analyst

1) Optical image characteristics may be accurately calculated in finite element analyses if the ray-intercept data is faithfully incorporated in the model by putting thermal and elastic nodes at each ray-intercept point. This has been shown to hold for the higher order effects (aberrations) as well[5].

2) Observe congruence between all the other thermal nodes and all the other elastic grid points.

3) In planning the elastic model's accuracy, consider the number of optical surfaces that will contribute to the image. The errors in the image characteristics may be bounded by multiplying the anticipated errors in the elastic displacements by the

number of free optical surfaces.

4) Be very careful in defining the nature of the heat load and its distribution. Provide adequate modeling geometry to be able to distribute the heat accurately and replicate the flux gradients that may exist in the real heating condition. This may dictate additional complexity and a finer mesh in the model but, ultimately, accurately modeling the heat loading conditions is essential to accurate predictions of its influence on the image characteristics.

6.0 CONCLUSIONS

Unified analysis provides the greatest opportunity for reducing the error and uncertainties which such analyses entail while making their sources understandable and tractable. A similar analysis using Integrated techniques would add errors and uncertainties from the translators, formatters, interpolators and extrapolators and their effects are extremely difficult to quantify, predict or control. The errors in the Unified analysis described above are knowable, predictable and controllable.

REFERENCES

1 "Optical Analog" is a trade mark of Alson E Hatheway Inc.
2. "Code V" is a trade mark of Optical Research Associates Inc
3. "MSC/NASTRAN is a trade mark of the MacNeal Schwendler Corp.
4 MSC/NASTRAN Application Manual, Section 5, Application Note of March 1984.
5 Hatheway, Alson E , "Optomechanical analysis strategies," *Structural Mechanics of Optical Systems II* (Bellingham, WA SPIE, 1987), pp. 96-103.